PNAS RESEARCH ARTICLE | ENVIRONMENTAL SCIENCES

Understanding the coevolution of mask wearing and epidemics: A network perspective

Zirou Qiu[a,b,1], Baltazar Espinoza[b], Vitor V. Vasconcelos[c,d,e,f], Chen Chen[b], Sara M. Constantino[f,g,h,i], Stefani A. Crabtree[j,k], Luojun Yang[l], Anil Vullikanti[a,b], Jiangzhuo Chen[b], Jörgen Weibull[m], Kaushik Basu[n,o], Avinash Dixit[p], Simon A. Levin[l,1], and Madhav V. Marathe[a,b,1]

Edited by Marcus Feldman, Stanford University, Stanford, CA; received December 29, 2021; accepted April 5, 2022

Nonpharmaceutical interventions (NPIs) such as mask wearing can be effective in mitigating the spread of infectious diseases. Therefore, understanding the behavioral dynamics of NPIs is critical for characterizing the dynamics of disease spread. Nevertheless, standard infection models tend to focus only on disease states, overlooking the dynamics of "beneficial contagions," e.g., compliance with NPIs. In this work, we investigate the concurrent spread of disease and mask-wearing behavior over multiplex networks. Our proposed framework captures both the competing and complementary relationships between the dueling contagion processes. Further, the model accounts for various behavioral mechanisms that influence mask wearing, such as peer pressure and fear of infection. Our results reveal that under the coupled disease–behavior dynamics, the attack rate of a disease—as a function of transition probability—exhibits a critical transition. Specifically, as the transmission probability exceeds a critical threshold, the attack rate decreases abruptly due to sustained mask-wearing responses. We empirically explore the causes of the critical transition and demonstrate the robustness of the observed phenomena. Our results highlight that without proper enforcement of NPIs, reductions in the disease transmission probability via other interventions may not be sufficient to reduce the final epidemic size.

epidemiology | social and behavioral contagions | multilayer networks | phase transitions | individual behavior

Significance

Nonpharmaceutical interventions such as mask wearing play a critical role in reducing disease prevalence. Under the dueling dynamics of mask wearing and disease, we observe a robust nonmonotonic relationship between the attack rate (i.e., the fraction of the ever-infected population) and the transmission probability of the disease. Specifically, the attack rate exhibits an abrupt reduction as the transmission probability increases to a critical threshold. Furthermore, we characterize regimes of the transmission probability where multiple waves of infection and mask adoption are expected. Our results highlight the necessity of continued public mask-wearing mandates to suppress the epidemic and effectively prevent its revival.

During pandemics, nonpharmaceutical interventions (NPIs) are among the most effective countermeasures to reduce infection rates and to contain the spread of diseases (1–3). The effectiveness of NPIs, which include mask wearing (4), frequent hand sanitizing, and social distancing (5, 6), have been thoroughly investigated (1–3, 7). In particular, extensive work has demonstrated the efficacy of mask usage against the dissemination of respiratory diseases (1, 8–10), and wearing masks has played a critical role in curtailing disease prevalence during the COVID-19 pandemic (11).

Wearing masks provides social benefits but also requires some degree of personal discomfort. Further, in many countries without a recent history of respiratory epidemics, wearing masks is an unfamiliar behavior whose efficacy is not well understood (12). In these contexts, it is thus unlikely that the population will adopt this prosocial behavior spontaneously. Instead, the decision to wear a mask has been shown to depend on risk perceptions, prosocial preferences, elite influence, and peer pressure (13–18). Formally, mask-wearing behavior can be described as a complex contagion whose adoption requires multiple social contacts with different sources (19). Complex contagion processes are commonly studied using threshold models (20, 21) where an individual adopts a behavior if the fraction of immediate connections engaging in the behavior exceeds a personal threshold (i.e., peer pressure effects). There is extensive literature on threshold models, with classic works including Granovetter's model of collective behavior (20) and Watts's global cascades model (22). Threshold models have also been studied in the diffusion of social influence (23), social conventions (24), public opinion (25), and social behaviors in general (26).

In this work, we propose a multicontagion framework that intertwines a threshold social contagion model with an epidemic model to investigate the interrelated dynamics between mask wearing and disease. For the social dynamics, individual-level decisions to wear masks are jointly determined by 1) peer pressure (13, 27, 28), 2) fear of the pandemic (29, 30), and 3) prosociality (31–33). The disease dynamics extend the susceptible-infected-recovered (SIR) model by accounting for the efficacy of mask wearing in decreasing the disease transmission rates. Given that the two types of contagions can spread through different social connections, we model the system using a two-layer network (34) over the same population, where each contagion spreads on a distinct layer simultaneously, as shown in Fig. 1. Overall, our model captures a bidirectional relationship between the dueling processes: 1) Wearing masks

Author contributions: Z.Q., B.E., V.V.V., C.C., S.M.C., S.A.C., L.Y., A.V., J.C., J.W., K.B., A.D., S.A.L., and M.V.M. designed research; Z.Q., B.E., V.V.V., C.C., S.M.C., S.A.C., L.Y., A.V., J.C., J.W., K.B., A.D., S.A.L., and M.V.M. performed research; and Z.Q., B.E., V.V.V., C.C., S.M.C., S.A.C., L.Y., A.V., J.C., J.W., K.B., A.D., S.A.L., and M.V.M. wrote the paper.

The authors declare no competing interest.

This article is a PNAS Direct Submission.

[1]To whom correspondence may be addressed. Email: zq5au@virginia.edu, marathe@virginia.edu, or slevin@princeton.edu.

This article contains supporting information online at https://www.pnas.org/lookup/suppl/doi:10.1073/pnas.2123355119/-/DCSupplemental.

Published June 22, 2022.

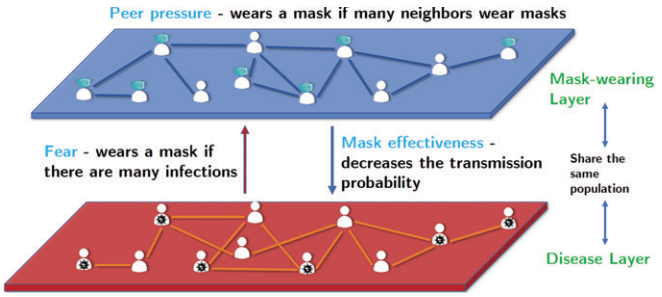

Fig. 1. A pictorial example of the proposed dueling contagion framework where the social contagion—mask wearing—spreads on the top layer, and the disease spreads on the bottom layer. The two layers share the same population.

reduces the transmission rates, and 2) increase in the disease prevalence triggers mask wearing. Further, our model can be extended to incorporate other prosocial behaviors that incur private costs and are likely subject to peer influences (e.g., vaccination or social distancing).

Main Findings

Under the joint dynamics of social and biological contagions, the fraction of the population that was ever infected by the end of the epidemic (i.e., the attack rate of the disease) exhibits a nonmonotonic critical transition (35, 36) as a function of the disease transmission probability p, characterized by two tipping points (37) (Fig. 2*A*). To our knowledge, this nonmonotonic phenomenon is not observed under existing models.* We further characterize two regimes of the disease transmission probabilities based on the tipping points, where multiple infection waves are expected only in the first regime. This result resembles the real-world oscillation of infection and mask usage in various states in the United States (e.g., the example of Virginia in *SI Appendix*, Fig. S1). In a series of experiments, we demonstrate the robustness of the observed phenomena over a wide range of network settings, model parameters, and extensions. We also observe the phenomena in an analogous mean-field model.

Our results suggest that in the presence of adaptive mask wearing, a less infectious disease may produce a higher attack rate than its more infectious counterparts. Subsequently, using traditional interventions that effectively decrease the infection rate—such as mass vaccination—without ensuring continued enforcement of NPIs may not be sufficient to reduce the final epidemic size. In the worst-case scenario, containment efforts may result in a larger final epidemic size if mask wearing is not continuously reinforced. Indeed, there was a resurgence of COVID-19 cases in the United States after vaccinations.† The number of new daily cases jumped by approximately an order of magnitude from early June 2021 to early September 2021.‡ Our results emphasize the importance of continued public mask-wearing mandates to effectively suppress the evolution of the epidemic and prevent its revival.

Experimental Settings and Design

Model Overview. We model the concurrent dissemination of mask-wearing behavior and disease on a two-layer network over the same population, where each contagion spreads on a single layer. Vertices in the network represent individuals, and the immediate connections of each individual, which we refer to as neighbors, are linked by edges. For the social dynamics, individuals update actions synchronously based on their neighbors' previous actions. Specifically, at each time step, an individual v wears a mask if and only if at least one of the following conditions is satisfied: 1) peer pressure, the fraction of neighbors wearing masks at the previous time step exceeds a personal threshold $\tau_1(v)$; 2) fear, the overall fraction of infected population in the previous time step exceeds a personal threshold $\tau_2(v)$; and 3) prosociality, v is a prosocial type, where prosociality is an indicator random variable that is assigned to each individual as an initial condition. Since prosocial individuals always wear masks, behavioral adaptations are limited to nonprosocial people. Overall, the social dynamics incorporate both global information based on the disease prevalence and local information based on neighbors' actions.

Our social contagion model can be seen as an extension of Watts's model (22), with the following key distinctions: 1) Watts's dynamics are irreversible—once an individual contracts the contagion (e.g., wears a mask), the adoption is permanent throughout the entire course of the dynamics. In contrast, the mask-wearing states are reversible under our model, such that a person chooses not to wear a mask at a time step if none of the three conditions above are satisfied. 2) Individuals update states in random asynchronous order under Watts's model, whereas our model considers a synchronous update scheme. 3) Our model further intertwines the social dynamics with the disease dynamics. Note that the first distinction already implies a significant difference between the two

*An overview of the existing models appears in *SI Appendix*.

†In addition to relaxation of NPIs, there are multiple possible explanations for the increasing cases mentioned here, including the spread of the delta variant and waning immunity. Improper enforcement of NPIs is just one of the factors contributing to the resurgence of COVID-19 cases.

‡Data from CDC: https://covid.cdc.gov/covid-data-tracker//#trends_dailytrendscases.

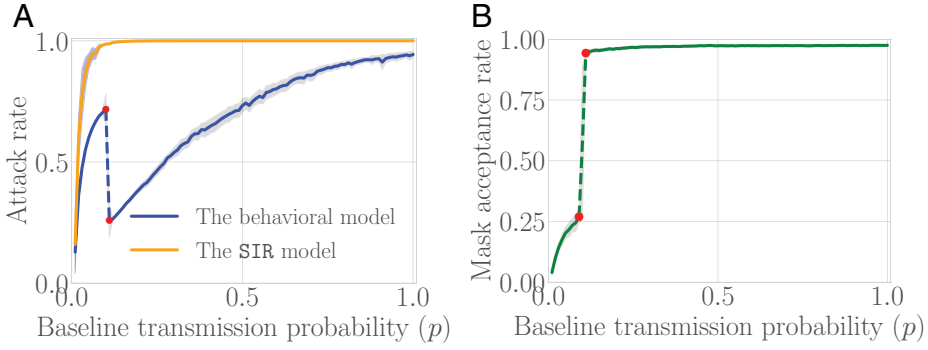

Fig. 2. Dueling dynamics of the behavioral model. (*A*) Contrasting the behavioral model with the SIR model. Shown is the attack rate as a function of the disease baseline transmission probability (p) for the behavioral model (blue line) and for the SIR model (orange line). (*B*) Social dynamics of the behavioral model. Shown is the mask acceptance rate as a function of p. The variances are shown as shaded regions, with one SD above and below the mean. The two tipping points for the behavioral model are highlighted in red. All parameters are set to their baseline values shown in Table 1.

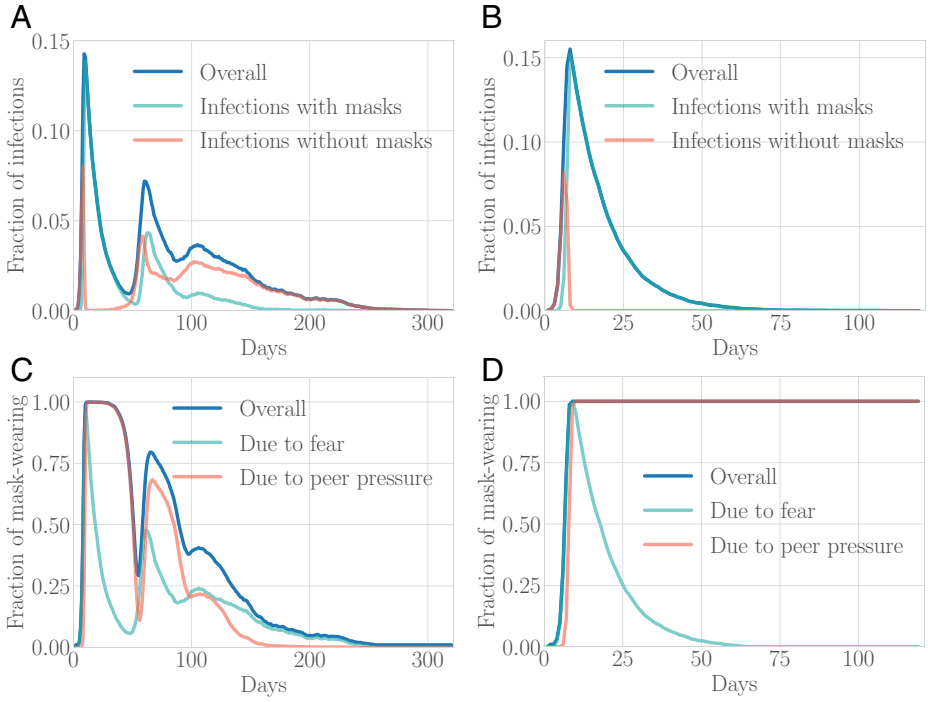

Fig. 3. The coevolution of disease and mask adoption at the tipping points. Shown are the disease and mask-wearing time-series dynamics, respectively. The baseline transmission probability is fixed to the value at the first/second tipping point. All other parameters are set to their baseline values shown in Table 1. (*A*) Disease dynamics at the first tipping point. (*B*) Disease dynamics at the second tipping point. (*C*) Mask dynamics at the first tipping point. (*D*) Mask dynamics at the second tipping point.

models. For example, the oscillation of mask wearing shown in Fig. 3 will not be observed if the dynamics are irreversible.

The disease dynamics combine the SIR model with the aforementioned social dynamics (Fig. 4). At the individual level, wearing masks dampens the probability of pairwise disease transmission, where the reduction factor depends on the mask-wearing states of both individuals. Further, a recovered individual gains permanent immunity. Our model accounts for both competing (i.e., wearing masks restrains the disease spread) and complementary (i.e., disease incentivizes mask wearing) dynamics between the contagions. We provide detailed model formulations in *SI Appendix*.

Baseline Parameters. The baseline values of our parameters are listed in Table 1. In general, the behavioral thresholds are heterogeneous. Peer pressure and fear thresholds are chosen from a uniform distribution in the range specified in Table 1. The detailed methodology for choosing these baseline values is given in *SI Appendix*.

Experimental Design. We numerically explore the dueling dynamics of the social and biological contagions. Let the disease baseline transmission probability p be the probability of infection for a susceptible individual in contact with an infected neighbor (per pairwise interaction), when both individuals do not wear masks. Note that p decreases if either the susceptible individual or the infected neighbor wears a mask. We focus on the attack rate as a measure of the disease's impact on the susceptible population. Further, we use the average fraction of people wearing masks per day to describe the strength of the behavioral response. Specifically, for each epidemic process, we record the following two results: 1) attack rate κ, the fraction of the population that was ever infected during the epidemic (45), and 2) the mask acceptance rate $\eta = \sum_i^d x_i/d$, where d is the number of time steps (e.g., days) a disease spreads in the population, and x_i is the random variable representing the fraction of the population wearing masks on the ith day.

Our numerical experiments investigate how the attack rate and the mask acceptance rate vary for diseases with different transmission probabilities. Each data point of a testing scenario is averaged over 100 initializations, where each initialization consists of 10 randomly selected individuals infected on day 1 and a new random two-layer network. We first conducted experiments on random scale-free networks of 30,000 vertices with average degrees of 10, generated using the Barabasi–Albert model (46). The two network

Table 1. Baseline parameters

Parameter	Description	Baseline value	Ref.
p_s	Fraction of prosocial population	0.01	Assumed
p_i	Fraction of population wearing masks on day 1 (i.e., zero infection)	0.00	Assumed
l_f	A lower bound of the threshold for fear	0.001	Assumed
u_f	An upper bound of the threshold for fear	0.15	Assumed
l_p	A lower bound of the threshold for peer pressure	0.3	(28, 38, 39)
u_p	An upper bound of the threshold for peer pressure	1.0	(40–42)
α	Discounting factor for a susceptible individual wearing a mask	0.3	(1, 9, 10, 43)
β	Discounting factor for an infected individual wearing a mask	0.1	(1, 9, 10, 43)
r	Recovery rate	1/9	(44)

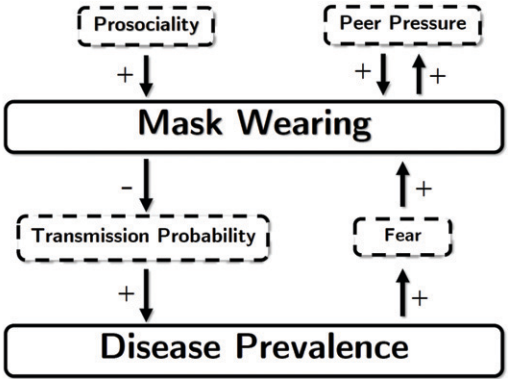

Fig. 4. Causation diagram for the dueling dynamics. The arrows indicate direct influences. The positive (+) and negative (–) signs imply positive and negative correlations, respectively.

layers are constructed under the same baseline scale-free network, where each layer undergoes random edge perturbations without altering the degree distributions (47).

To further study the robustness of our results, we perform simulations over a wide range of model parameters and network structures. In particular, we conducted experiments on Erdös–Rényi random graphs (48) of sizes up to 100,000 with different average degrees and scale-free networks with exponents from 2.35 to 3.39. We also vary the social and disease parameters (e.g., fraction of the prosocial population, ranges of peer pressure thresholds and fear thresholds, etc.) to investigate their influences on the dueling dynamics.

Results

Dueling Social and Biological Dynamics Induce a Critical Transition. We begin by contrasting the disease dynamics between our behavioral model and the SIR model shown in Fig. 2*A*. For the SIR model, we observe a monotonic increase of the attack rate as the disease baseline transmission probability p increases. In contrast, the attack rate under the behavioral model exhibits a critical transition characterized by tipping points. Specifically, in phase one, the attack rate increases as the disease becomes more infectious, peaking at the first tipping point. As p exceeds the first tipping point, the attack rate reduces sharply and enters the second phase. For clearness of demonstration, we refer to the point where the second phase begins as the second tipping point. Numerically, we can capture the two tipping points with a finer granularity such that the critical transition happens abruptly and the function exhibits a discontinuity.

We further investigate the sensitivity of the results to the initial conditions and the randomness of the networks. Overall, we observe a low variance in the simulation results for the behavioral model. More importantly, the shape of the variance region displays a similar critical transition to that of the mean data line, as shown in Fig. 2*A*.[§]

The critical transition on the attack rate in the behavioral model suggests that a less transmissible disease could infect a broader range of the population than some more infectious diseases. To better understand this phenomenon, Fig. 2*B* depicts the population's behavioral responses during the epidemic period, given by the mask acceptance rate, as a function of p. Specifically, the social dynamics also exhibit a critical transition with two tipping points. Further, the transmission probabilities that determine the two tipping points for the disease dynamics correspond to those for the social dynamics. Intuitively, the high attack rate at the first tipping point induces a steep increase in mask acceptance rate, which in turn triggers a sharp decrease in the attack rate to the second tipping point. Overall, the two critical transitions are intertwined.

We further study the robustness of the critical transition with respect to 1) model parameters, a) fear and peer pressure thresholds, b) mask effectiveness, and c) the fraction of prosocial individuals; 2) network topology, a) Erdös–Rényi, b) power law, and c) real-world networks; and 3) model extensions, a) habit formation around mask wearing and b) presence of asymptomatic infections. Overall, the critical transition occurs under a wide spectrum of system and parameter settings. See *SI Appendix* for a detailed analysis.

The observed critical transitions can classify a disease's baseline transmission probability into two regimes: 1) up to the first tipping point (i.e., the first regime) and 2) at the second tipping point and onward (i.e., the second regime). For simplicity, we refer to a disease as a first- (second-)regime disease if its transmission probability falls in the first (second) regime. The subsequent sections explore the nature of critical transitions based on the two regimes.

Causes of the Critical Transition: The Trade-off between Prevalence Peak and Disease Persistence. We show that under the behavioral model, a first-regime disease survives longer than a second-regime disease, thereby infecting more total people and producing a higher attack rate than some diseases in the second regime. Following the literature (49, 50), we define the duration of the epidemic to be the number of time steps (e.g., days) between the first infection and a complete absence of the disease in the population. Note that the duration of an epidemic is a random variable whose probability distribution depends on the population size.[¶] Let the disease prevalence peak denote the largest population share of infected individuals on a single day over the epidemic period. The duration and the disease prevalence peak capture the persistence and infectiousness of disease, respectively.

Fig. 5*A* shows the epidemic duration and the disease prevalence peak as functions of the baseline transmission probability p. In Fig. 5*A*, the duration exhibits a critical transition as p increases, characterized by the same tipping points as those in Fig. 2. Specifically, we see a sharp decrease in the duration as p exceeds the first tipping point. This result is consistent with the simulations reported in Fig. 2 such that before the first tipping point, mask-wearing rates remain low, thus allowing the disease to propagate for long periods. In contrast, after the second tipping point, mask-wearing rates become high, quickly eradicating the epidemic.

Fig. 5*B* shows a positive monotonic correlation between the disease prevalence peak and p. Combined with Fig. 2, our simulations highlight the critical role of the population's behavioral response on the disease dynamics. In general, a disease in the second regime can infect a high fraction of the population in a short period, but it also diminishes quickly due to large and sustained mask-wearing responses. In contrast, a disease in the first regime produces a relatively low prevalence peak, which does not trigger sustained large-scale mask adoption. Therefore, by

[§]We omit the variance region in some of the future plots for the cleanness of the demonstration.

[¶]Alternatively, we can define the duration as the length of the shortest random time span of the disease after which the population share remains below a given threshold $\epsilon > 0$. Observe that the two definitions coincide when $\epsilon < 1/n$, where n is the population size. We remark that the critical transition shown in Fig. 5 will persist under this alternative definition of duration for low ϵ values.

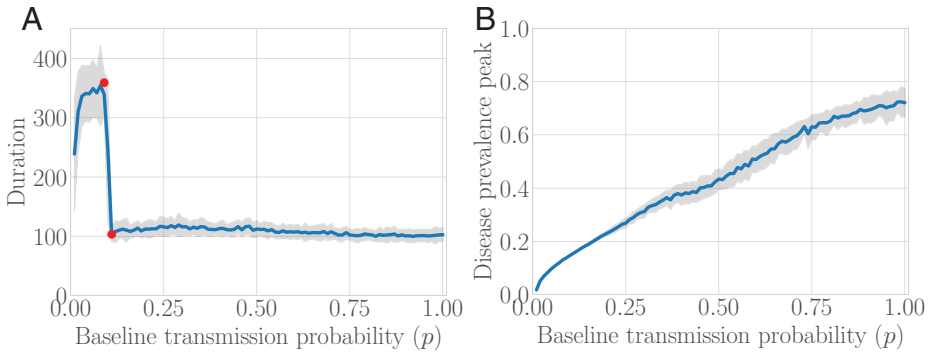

Fig. 5. Epidemic duration and the disease prevalence peak as functions of the baseline transmission probability p. (*A*) Epidemic duration as a function of p. Shown is a critical transition of the epidemic duration as the disease becomes more infectious. (*B*) Disease prevalence peak sizes as a function of p. Shown is a monotonic increase of the disease prevalence peak as p increases. The tipping points of the critical transition are highlighted in red in *A*. The variance is shown as a shaded region. All parameters are set to their baseline values shown in Table 1.

surviving for a much longer time, a first-regime disease could infect more people in the long run and thus produces a higher attack rate than some diseases in the second regime. The results provide key insights into the critical transition and illustrate the trade-off between the disease prevalence peak and persistence. We further highlight that when the transmission probability of a second-regime disease is high enough, even if it has a short duration, it can still produce an attack rate higher than under any diseases in the first regime. This can be seen in the upper half of the second regime in Fig. 2, which bypasses the attack rates in the first regime.

A Further Look at the Causes of the Critical Transition: Waves of Infections and Mask Adoptions. We further investigate the mechanisms driving the critical transition where we analyze the time-series dynamics of infections and mask adoptions under transmission probabilities p in the two regimes. We show that when p is in the first regime, the dueling dynamics incur multiple waves of infection and mask adoptions, resulting in a long epidemic duration. In contrast, when p surpasses the first tipping point, the disease prevalence peak exceeds a critical threshold that results in a sustained mask adoption, and the dueling dynamics exhibit single waves with short duration.

At each time step of our simulations, we record the fraction (normalized over the population size) of 1) currently active infections, 2) infected individuals with masks, and 3) infected individuals without masks. Moreover, we track the fraction of 1) the population wearing masks, 2) mask-wearing people incentivized by fear, and 3) mask-wearing people incentivized by peer pressure.

Multiple infection waves in the first regime. We set p to a value in the first regime and study how the fraction of infection and mask usage changes as the epidemic evolves. Fig. 3 *A* and *C* illustrates the joint dynamics that exhibit multiple waves of infection and mask adoption when p is at the first tipping point. Specifically, an initial rise in the disease prevalence sets off a drastic increase in mask usage due to fear. Since wearing masks decreases the pairwise transmission probability, this surge in mask wearing then triggers the disease curve to go down, resulting in a decrease of fear in the population. When p is in the first regime, however, the mask-wearing group cannot be sustained by peer pressure alone because the peer pressure thresholds of many mask-wearing individuals are not satisfied (i.e., wearing masks only because of fear). Consequently, mask prevalence drops due to the decrease in the level of fear as the risk of infection dissipates, resulting in a resurgence of the disease that infects the susceptible individuals who were previously protected by masks.

We observe that the decline in mask prevalence is smoother than the decline in the disease prevalence. This is due to peer pressure being a local mechanism; thus, it takes time for the abandonment of mask wearing to propagate across the network. Also, each infection wave is less pronounced than the preceding wave. This diminishing magnitude can be explained by the progressive recovery process and our assumption of permanent immunity: As time passes, more people are infected and recover, and there fewer susceptibles. It is essential to recognize that the usage or nonusage of masks may have causations devoid of the ground realities of the disease prevalence. When many people wear masks, the stigma for not wearing masks becomes high, triggering an increase in mask prevalence. When few wear masks, however, the stigma tends to be low, reinforcing the low incidence of mask wearing.

We further explore the joint dynamics under varying transmission probabilities sampled in the first regime where we observe qualitatively similar multiwaves of infection and mask adoption for all samples. Note that the oscillating dynamics in the first regime elaborate on the result shown in Fig. 5*A*, such that a disease in the first regime is more persistent because the epidemic undergoes multiple revivals. This contrasts to diseases in the second regime that die out after a single wave of infection, as shown in the next section.

Single infection waves in the second regime. We explore the time-series dynamics when p falls in the second regime. In the example shown in Fig. 3 *B* and *D* where p is at the second tipping point, we observed only a single wave of infection and mask adoption. In particular, as the disease initially spreads, its prevalence level crosses a critical threshold that triggers a large mask-wearing group such that peer pressure can then sustain mask wearing, as shown in Fig. 3*D*. This saturated behavioral response prevents the disease from resuscitating. As a result, the disease diminishes in a short time relative to disease duration in the first regime. We consistently observed qualitatively similar single-wave dynamics for all sampled transmission probabilities in the second regime.

In general, the contrast in the dueling dynamics of the two regimes (i.e., multiwave vs. single wave) occurs as a consequence of the distinctive behaviors at the peak of the mask dynamics, shown in Fig. 3 *C* and *D*, respectively. Notably, when p is in the first regime, mask usage deviates from the peak, allowing disease revival. On the other hand, mask usage converges at the peak when p is in the second regime. Our numerical experiments suggest that as p exceeds the first tipping point, the corresponding disease prevalence peak crosses a critical threshold, such that the number of the resulting mask-wearing people is large enough (i.e., also crosses a critical threshold) to be sustained by peer pressure (in the example in Fig. 3*D*, 100% of the population wear masks at the peak), resulting in a convergence of mask dynamics at the peak that averts future epidemic waves. Inversely, such a prevalence threshold is not met when p is in the first regime, thereby allowing

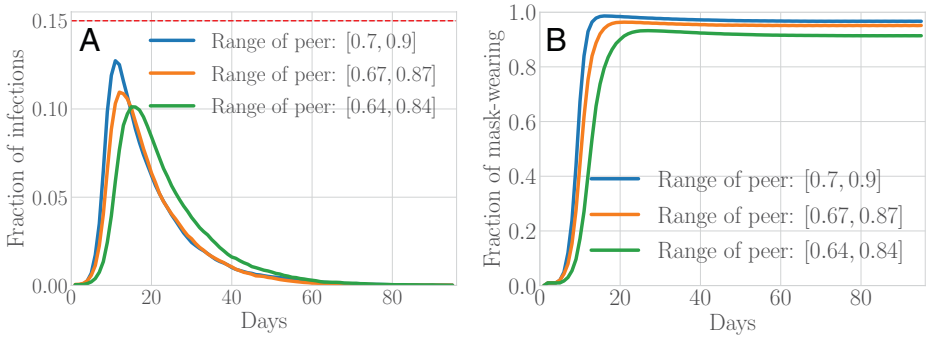

Fig. 6. The time-series dynamics at the second tipping point under varying ranges of peer pressure. (*A*) Disease dynamics at the second tipping point. (*B*) Mask dynamics at the second tipping point. *A* and *B* depict the infection and mask-wearing dynamics, respectively, for p fixed at the second tipping point, where the range of peer thresholds varies. The upper bound on the fear threshold is indicated in *A* with a dashed line.

mask usage to diminish from the peak, leading to multiwave infection.[‖] Critical phenomena are not uncommon in complex systems One classic example is Watts's model (22) (where adoption of contagion is irreversible) where the system incurs either minuscule or large cascades, with no middle-sized cascades. Nevertheless, given the difference between our social dynamics and Watts's dynamics, the existence of a similar critical phenomenon also in our model is interesting, as our social dynamics are reversible. We plan to further investigate this in future work. We highlight that the exact value at the convergence depends on the parameter setting, and the mask dynamics do not always anchor at 100%, as shown in Fig. 6.

The combined effect of these mechanisms explains the drastic difference in duration between a first-regime disease and a second-regime disease, which then produces the observed critical transition. We further demonstrate the robustness of the contrasting dynamics between the two regimes with respect to parameter settings in *SI Appendix*.

Enforcement of Mask Wearing Tames Epidemic Waves. In our model, the primary cause of multiwave infections is people's negligence after disease prevalence decreases, which then allows for the revival of the disease. Specifically, we observe diminishing mask wearing in the population after each reduction in the disease prevalence. We further explore the infection dynamics under a simple setting of public mask-wearing mandates: When the disease prevalence starts to lessen, we enforce mask-wearing individuals to continue wearing masks despite the reduction in peer pressure and fear. Subsequently, as shown in *SI Appendix*, Fig. S18, we can effectively suppress the revival of the disease and bring the anticipated oscillation of infection down to only a single wave. This observation highlights the importance of continuing mask mandates even under low disease prevalence and social stigma.

Mean-Field Model Analogy. Beyond exploring the critical transition on different network structures, we also investigate the emergence of the critical transition on an analogous mean-field model. In particular, mask wearing is incentivized by 1) peer pressure as a contagion process and 2) fear as a prevalence threshold condition (τ). Our mean-field model assumes a population composed of two risk groups: those who comply with public health recommendations and those who do not. We do not explicitly model prosociality, since individuals can switch across risk groups. Our model assumes that at an early stage, the epidemic evolves in the absence of behavioral responses; that is, at the beginning of the epidemic, the majority of the population does not comply with control policies. After the epidemic hits the prevalence threshold condition, the behavioral responses begin. In particular, people from the noncompliant group start to adopt precautionary behaviors, moving to the compliant group at a rate φ.

For simplicity, we assume the compliance adoption to be the same regardless of an individual's health status. We found that the qualitative behavior observed on the attack rate is sensitive, but remains robust to changes in the behavioral response strength. The detailed formulation of the mean-field model can be found in *SI Appendix*. Our results show the emergence of a similar critical transition on the attack rate as a function of the disease baseline transmission probability (p). In contrast to the network model, we note that for the mean-field model, the fear threshold condition alone is capable of producing the critical transition phenomena, whereas peer pressure alone is not capable of producing the critical transition. In Fig. 7, we show the attack rate as a function of the disease baseline transmission probability (p), for varying prevalence thresholds (τ). Note that in the selected simulations, the mean-field model exhibits only the first tipping point, which is produced by individuals moving from the noncompliant group to the compliant one.

Moreover, it is possible to formally incorporate individualized behavioral mechanisms—peer pressure and fear thresholds—on a mean-field model. To do so, the model formulation assumes individuals' randomly distributed independent peer pressure and fear thresholds. Consequently, the proposed mean-field model is equivalent to assuming a complete network. By tracking the corresponding cumulative distributions, we can track the fraction of mask wearers in the population $[m^*(I)]$. Consistent with the network model dynamics, we show that by explicitly incorporating individuals' behavioral thresholds, it is possible to characterize mask adoption dynamics. Particularly, we show the conditions under which the fraction of mask wearers in the population converges to a boundary limit state $[m^*(I) = 0$ or $m^*(I) = 1]$ and the conditions under which mask adoption undergoes hysteresis, assuming timescales separation. The detailed model formulation and additional results appear in *SI Appendix*.

Discussion

Intuitively, a disease with a lower transmission probability should produce a lower attack rate relative to a more infectious disease. In this work, however, we show that under the concurrent dynamics of mask-wearing behavior, a less infectious disease could cause a higher attack rate than its more infectious counterparts. This observation is captured by a critical transition of the attack rate

[‖] In Fig. 3, the percentage of mask adoption at the peak is 99.53%, with roughly 140 people not wearing masks. However, note that the exact number is not of interest.

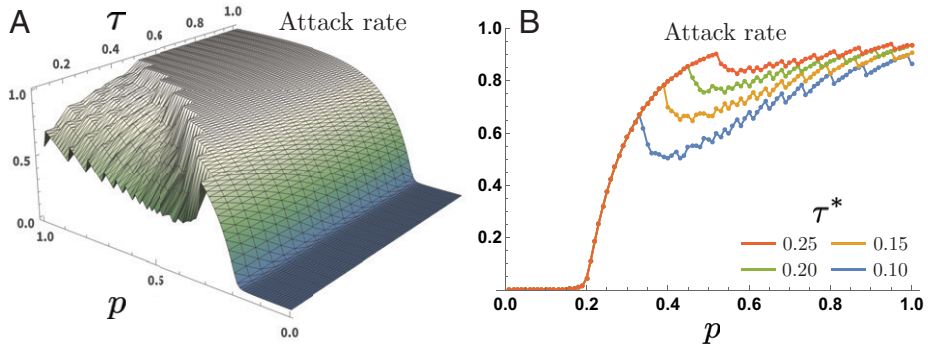

Fig. 7. Mean-field model critical transition. Unlike the network model, the global condition of fear, triggered at a prevalence threshold, produces the critical transition. (*A*) Mean-field model attack rate as a function of the disease baseline transmission probability (p), and the fear prevalence threshold (τ), for behavioral response $\varphi = 0.3$. (*B*) Selected simulations of the attack rate as a function of the disease baseline transmission probability (p), for fear prevalence threshold values $\tau = 0.1, 0.15, 0.2$, and 0.25 and behavioral response $\varphi = 0.3$.

as the disease transmission probability p increases, such that the attack rate abruptly reduces when p exceeds a tipping point. This finding points out that the pervasiveness of a disease is sometimes not reducible to its infectiousness. Thus, one should take precautions and use NPIs even when a disease is seemingly not too infectious. From a public health perspective, our simulations suggest that reducing the infection rate through control policies poses a paradox. In particular, interventions (e.g., vaccination) that decrease the disease's transmission probability are expected to lessen the epidemic burden. However, when there are adaptive behavioral responses, our simulations suggest that containment efforts may result in a larger final epidemic size if mask wearing is not continuously reinforced. Our results point to two distinct regimes of disease control: 1) Up to the first tipping point, any reduction of the infection probability leads to a reduction in the attack rate, and 2) from the second tipping point onward, there is an interval during which control policies may increase the attack rate if NPIs are not continuously enforced. An example of such an interval is shown in Fig. 8. Our findings have implications for public health policy by showing the importance of a sustained mask mandate to prevent a resurgence in disease prevalence.

Throughout the pandemic conflicting information has influenced peoples' decisions to wear (or not wear) masks. For example, an individual may internalize public health messages about the importance of wearing masks but live in a region where mask wearing has become politicized. In these instances, mandatory policies may be an essential avenue for ensuring widespread mask wearing in the face of countervailing social forces. Our model could serve as a basic framework to further investigate the effectiveness of NPI policies under the dueling dynamics of the population's behavioral response and disease. Finally, studies of complex systems have repeatedly shown our intuition is often incorrect. Particularly, understanding the effect of control policies also requires us to address potential unintended consequences.

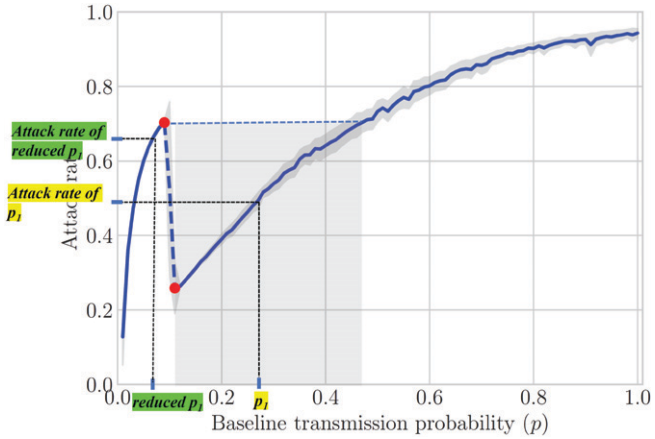

Fig. 8. The interval in the second regime. The shaded region depicts the interval of the transmission probability p where a reduction of p may lead to an increased attack rate. Specifically, p_1 denotes the baseline transmission of a disease (highlighted in yellow), and its reduced transmission probability is highlighted in green. Clearly, the reduction of p_1 leads to a higher attack rate.

Data Availability. Anonymized network files and source code data have been deposited in GitHub (https://github.com/BridgelessAlexQiu/Mask-Disease-Multilayer) and Zenodo (https://zenodo.org/record/6505964#.Yo_mPZPMJq8). All study data are included in this article and/or *SI Appendix*.

ACKNOWLEDGMENTS. We thank the anonymous reviewers for the helpful comments that substantially improved this paper. We thank members of the Biocomplexity COVID-19 Response Team and the Network Systems Science and Advanced Computing Division for their thoughtful comments and suggestions related to epidemic modeling and response support. We thank members of the Biocomplexity Institute and Initiative, University of Virginia, for useful discussion and suggestions. This work was partially supported by NIH Grant 1R01GM109718, NSF BIG DATA Grant IIS-1633028, NSF Grant OAC-1916805, NSF Expeditions in Computing Grants CCF-1918656 and CCF-1917819, NSF RAPID CNS-2028004, NSF RAPID OAC-2027541, NSF RAPID SES-DRMS-2030800, US Centers for Disease Control and Prevention 75D30119C05935, University of Virginia Strategic Investment Fund Award SIF160, Defense Threat Reduction Agency (DTRA) under Contract HDTRA1-19-D-0007, The James S. McDonnell Foundation 21st Century Science Initiative Collaborative Award in Understanding Dynamic and Multiscale Systems, the C3.ai Digital Transformation Institute and Microsoft Corporation, Gift from Google LLC, and the NSF (CNS-2027908 and CCF1917819), PREPARE: NSF Grant CNS-2041952, NSF RAPID Grant 2142997, The Jan Wallander and Tom Hedelius Research Foundation Grant P21-0052, The Coalition for Archaeological Synthesis, The Australian Research Council Grant LP200300886, and Virginia Department of Health (VDH) Grant PV-BII VDH COVID-19 Modeling Program Grant VDH-21-501-0135. Any opinions, findings, and conclusions or recommendations expressed in this material are those of the author(s) and do not necessarily reflect the views of the funding agencies.

Author affiliations: [a]Department of Computer Science, University of Virginia, Charlottesville, VA 22904; [b]Network Systems Science and Advanced Computing Division, Biocomplexity Institute, University of Virginia, Charlottesville, VA 22904; [c]Informatics Institute, University of Amsterdam, 1098 XH Amsterdam, The Netherlands; [d]Institute for Advanced Study, University of Amsterdam, 1012 GC Amsterdam, The Netherlands; [e]Princeton Institute for International and Regional Studies, Princeton University, Princeton, NJ 08544; [f]Andlinger Center for Energy and the Environment, Princeton University, Princeton, NJ 08540; [g]School of Public Policy and Urban Affairs, Northeastern University, Boston, MA 02115; [h]School of Public and International Affairs, Princeton University, Princeton, NJ 08540; [i]Department of Psychology, Northeastern University, Boston, MA 02115; [j]Department of Environment and Society, Utah State University, Logan, UT 84322; [k]The Santa Fe Institute, Santa Fe, NM 87501; [l]Department of Ecology and Evolutionary Biology, Princeton University, Princeton, NJ 08540; [m]Department of Economics, Stockholm School of Economics, SE-113 83 Stockholm, Sweden; [n]Department of Economics, Cornell University, Ithaca, NY 14853; [o]S. C. Johnson College of Business, Cornell University, Ithaca, NY 14853; and [p]Department of Economics, Princeton University, Princeton, NJ 08544

1. S. E. Eikenberry *et al.*, To mask or not to mask: Modeling the potential for face mask use by the general public to curtail the COVID-19 pandemic. *Infect. Dis. Model.* **5**, 293–308 (2020).
2. N. Ferguson *et al.*, Report 9: Impact of non-pharmaceutical interventions (NPIs) to reduce COVID19 mortality and healthcare demand. *Imp. Coll. Lond.* **10**, 491–497 (2020).
3. S. Lai *et al.*, Effect of non-pharmaceutical interventions to contain COVID-19 in China. *Nature* **585**, 410–413 (2020).
4. M. H. Haischer *et al.*, Who is wearing a mask? Gender-, age-, and location-related differences during the COVID-19 pandemic. *PLoS One* **15**, e0240785 (2020).
5. M. Farboodi, G. Jarosch, R. Shimer, Internal and external effects of social distancing in a pandemic. *J. Econ. Theory* **196**, 105293 (2021).
6. F. M. Toxvaerd, "Equilibrium social distancing" (Cambridge Working Papers in Economics, Faculty of Economics, University of Cambridge, 2020). https://www.repository.cam.ac.uk/bitstream/handle/1810/305407/cwpe2021.pdf?sequence=1. Accessed 2 June 2022.
7. S. Flaxman *et al.*; Imperial College COVID-19 Response Team, Estimating the effects of non-pharmaceutical interventions on COVID-19 in Europe. *Nature* **584**, 257–261 (2020).
8. V. C. C. Cheng *et al.*, The role of community-wide wearing of face mask for control of coronavirus disease 2019 (COVID-19) epidemic due to SARS-CoV-2. *J. Infect.* **81**, 107–114 (2020).
9. N. H. L. Leung *et al.*, Respiratory virus shedding in exhaled breath and efficacy of face masks. *Nat. Med.* **26**, 676–680 (2020).
10. R. B. Patel, S. D. Skaria, M. M. Mansour, G. C. Smaldone, Respiratory source control using a surgical mask: An in vitro study. *J. Occup. Environ. Hyg.* **13**, 569–576 (2016).
11. J. Howard *et al.*, An evidence review of face masks against COVID-19. *Proc. Natl. Acad. Sci. U.S.A.* **118**, e2014564118 (2021).
12. L. Peeples, What the data say about wearing face masks. *Nature* **586**, 186–189 (2020).
13. M. DeJonckheere, M. Waselewski, X. Amaro, A. Frank, K. P. Chua, Views on COVID-19 and use of face coverings among US youth. *J. Adolesc. Health* **68**, 873–881 (2021).
14. E. Goffman, *Stigma: Notes on the Management of Spoiled Identity* (Simon and Schuster, 2009).
15. F. N. Santana, S. L. Fischer, M. O. Jaeger, G. Wong-Parodi, Responding to simultaneous crises: Communications and social norms of mask behavior during wildfires and COVID-19. *Environ. Res. Lett.* **15**, 111002 (2020).
16. S. Pfattheicher, L. Nockur, R. Böhm, C. Sassenrath, M. B. Petersen, The emotional path to action: Empathy promotes physical distancing and wearing of face masks during the COVID-19 pandemic. *Psychol. Sci.* **31**, 1363–1373 (2020).
17. P. Campos-Mercade, A. N. Meier, F. H. Schneider, E. Wengström, Prosociality predicts health behaviors during the COVID-19 pandemic. *J. Public Econ.* **195**, 104367 (2021).
18. A. Lindbeck, S. Nyberg, J. W. Weibull, Social norms and economic incentives in the welfare state. *Q. J. Econ.* **114**, 1–35 (1999).
19. D. Centola, M. Macy, Complex contagions and the weakness of long ties. *Am. J. Sociol.* **113**, 702–734 (2007).
20. M. Granovetter, Threshold models of collective behavior. *Am. J. Sociol.* **83**, 1420–1443 (1978).
21. D. Guilbeault, J. Becker, D. Centola, "Complex contagions: A decade in review" in *Complex Spreading Phenomena Social Systems*, S. Lehmann, Y. Y. Ahn, Eds. (Springer, Cham, Switzerland, 2018), pp. 3–25.
22. D. J. Watts, A simple model of global cascades on random networks. *Proc. Natl. Acad. Sci. U.S.A.* **99**, 5766–5771 (2002).
23. P. S. Dodds, D. J. Watts, A generalized model of social and biological contagion. *J. Theor. Biol.* **232**, 587–604 (2005).
24. M. Ye *et al.*, Collective patterns of social diffusion are shaped by individual inertia and trend-seeking. *Nat. Commun.* **12**, 5698 (2021).
25. D. J. Watts, P. S. Dodds, Influentials, networks, and public opinion formation. *J. Consum. Res.* **34**, 441–458 (2007).
26. M. Gladwell, *The Tipping Point: How Little Things Can Make a Big Difference* (Little, Brown, 2006).
27. F. V. Hansstein, F. Echegaray, Exploring motivations behind pollution-mask use in a sample of young adults in urban China. *Global. Health* **14**, 122 (2018).
28. E. J. Van Leeuwen, D. B. Haun, Conformity without majority? The case for demarcating social from majority influences. *Anim. Behav.* **96**, 187–194 (2014).
29. K. M. Fitzpatrick, C. Harris, G. Drawve, Fear of COVID-19 and the mental health consequences in America. *Psychol. Trauma.* **12**, S17–S21 (2020).
30. S. Taylor, *The Psychology of Pandemics: Preparing for the Next Global Outbreak of Infectious Disease* (Cambridge Scholars Publishing, 2019).
31. K. Aquino, A. Reed II, The self-importance of moral identity. *J. Pers. Soc. Psychol.* **83**, 1423–1440 (2002).
32. C. H. Declerck, C. Boone, G. Emonds, When do people cooperate? The neuroeconomics of prosocial decision making. *Brain Cogn.* **81**, 95–117 (2013).
33. J. Nai, J. Narayanan, I. Hernandez, K. Savani, People in more racially diverse neighborhoods are more prosocial. *J. Pers. Soc. Psychol.* **114**, 497–515 (2018).
34. M. Kivelä *et al.*, Multilayer networks. *J. Complex Netw.* **2**, 203–271 (2014).
35. D. Balcan, A. Vespignani, Phase transitions in contagion processes mediated by recurrent mobility patterns. *Nat. Phys.* **7**, 581–586 (2011).
36. M. Scheffer, "Terrestrial ecosystems" in *Critical Transitions in Nature and Society*, S. A. Levin, S. H. Strogatz, Eds. (Princeton University Press, 2020), pp. 216–239.
37. T. C. Schelling, Dynamic models of segregation. *J. Math. Sociol.* **1**, 143–186 (1971).
38. M. Wolf, R. H. Kurvers, A. J. Ward, S. Krause, J. Krause, Accurate decisions in an uncertain world: Collective cognition increases true positives while decreasing false positives. *Proc. Biol. Sci.* **280**, 20122777 (2013).
39. D. Guilbeault, D. Centola, Topological measures for identifying and predicting the spread of complex contagions. *Nat. Commun.* **12**, 4430 (2021).
40. L. He *et al.*, Why do people oppose mask wearing? A comprehensive analysis of US tweets during the COVID-19 pandemic. *J. Am. Med. Inform. Assoc.* **28**, 1564–1573 2021).
41. L. H. Kahane, Politicizing the mask: Political, economic and demographic factors affecting mask wearing behavior in the USA. *East. Econ. J.* **47**, 1–21 (2021).
42. A. Millie, *Anti-Social Behaviour* (McGraw-Hill Education, United Kingdom, 2008).
43. C. R. MacIntyre *et al.*, The efficacy of medical masks and respirators against respiratory infection in healthcare workers. *Influenza Other Respir. Viruses* **11**, 511–517 (2017).
44. R. Wölfel *et al.*, Virological assessment of hospitalized patients with COVID-2019. *Nature* **581**, 465–469 (2020).
45. J. E. Matthews *et al.*, The epidemiology of published norovirus outbreaks: A review of risk factors associated with attack rate and genogroup. *Epidemiol. Infect.* **140**, 1161–1172 (2012).
46. A. L. Barabási, R. Albert, Emergence of scaling in random networks. *Science* **286**, 509–512 (1999).
47. M. E. Newman *et al.*, "Random graphs as models of networks" in *Handbook of Graphs and Networks: From the Genome to the Internet*, S. Bornholdt, H. G. Schuster, Eds. (Wiley, 2003), pp. 35–68.
48. P. Erdos *et al.*, On the evolution of random graphs. *Publ. Math. Inst. Hung. Acad. Sci* **5**, 17–60 (1960).
49. L. J. Allen, "An introduction to stochastic epidemic models" in *Mathematical Epidemiology*, F. Brauer, P. V. D. Driessche, J. Wu, Eds. (Springer, 2008), pp. 81–130.
50. A. D. Barbour, The duration of the closed stochastic epidemic. *Biometrika* **62**, 477–482 (1975).